Proceedings of 2013 IEEE
International Conference on Mechatronics and Automation
August 4 - 7, Takamatsu, Japan

Dynamic Reconfiguration Manipulability Analysis of Redundant Robot

Taoran Feng, Yosuke Kobayashi, Mamoru Minami and Akira Yanou
Graduate School of Natural Science and Technology
Okayama University
Okayama, Japan
{*touzen, kobayashi2, minami, yanou*}*@suri.sys.okayama-u.ac.jp*

***Abstract*— In this paper, we propose a new index inspired by dynamic manipulability for redundent robot proposed by Yoshikawa to estimate dynamic ability to change configuration by using remaining redundancy, while prior task is controlled, for example, end-effectors being controlled to a desired trajectory in task space. Several indexes have been proposed so far to measure statical and dynamical capability of robot manipulator. For example, Dynamic Manipulability Ellipsoid (DME) describes a distribution of hand acceleration produced by normalized joint torque. Besides, Reconfiguration Manipulability Ellipsoid (RME) denotes a distribution of each link velocity produced by joint angular velocity. In this paper, we proposed a new concept named Dynamic Reconfiguration Manipulability (DRM) which combined dynamic manipulability with reconfiguration manipulability, and we examined and analyzed it through simulations to test and verify its validity and usefulness.**

***Index Terms*— Dynamic, reconfiguration, acceleration.**

I. Introduction

A variety of researches that discussed about performance of robot manipulators were extended from the middle of 1980's to the end of 1990's. For example, manipulability that use kinematics to show the relationship between joints' angles and tip's velocity of end-link[1], and Dynamic Manipulability that considering dynamic equation's condition to show relationship between joints' torque and tip's acceleration of end-link[2][3]. To evaluate these manipulabilities, ellipsoids are used showing velocity's directions and values. On the other hand, Reonfiguration Manipulability of redundant manipulators was proposed using kinematics to indicate intermediate links' manipulabilities[4], and its usefulness to obstacle avoidance and singular configuration avoidance had been improved. However, as is well-known, with the increase of degrees of redundant manipulators, weights are also increasing. So, in this situation, it is not suitable for only basing on kinematics when high-accuracy control is required. Therefore, we propose a new concept Dynamic Reconfiguration Manipulability(DRM) which is a measure of how much a dynamical system can potentially produce a motion in a workspace with normalized input torque, by combining the Dynamic Manipulability with Reconfiguration Manipulability. This new measure represents how much the dynamical system of robots possesses shape-reconfiguration acceleration ability in workspace by unit torque input for all joints during executing primary tasks. In this paper, we propose the concept of DRM, and prove physical properties, validity and usefulness of DRM using 4 links manipulator in 2-dimensional space.

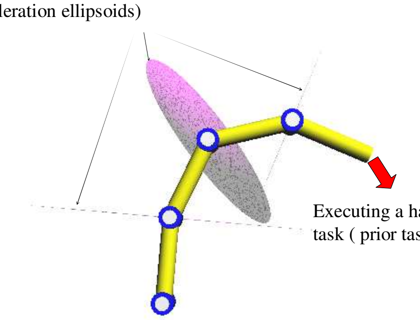

Fig. 1. Application of Dynamic Reconfiguration Manipulability for redundant manipulator

II. Dynamic Reconfiguration Manipulability

A. Dynamic Manipulability

In general, equation of dynamics for serial link manipulators is written as

$$\boldsymbol{M}(\boldsymbol{q})\ddot{\boldsymbol{q}} + \boldsymbol{h}(\boldsymbol{q},\dot{\boldsymbol{q}}) + \boldsymbol{g}(\boldsymbol{q}) + \boldsymbol{D}\dot{\boldsymbol{q}} = \boldsymbol{\tau} \qquad (1)$$

where $\boldsymbol{M}(\boldsymbol{q}) \in \mathrm{R}^{n\times n}$ is inertia matrix, $\boldsymbol{h}(\boldsymbol{q},\dot{\boldsymbol{q}}) \in \mathrm{R}^{n}$ and $\boldsymbol{g}(\boldsymbol{q}) \in \mathrm{R}^{n}$ are vectors which indicate Coriolis force, centrifugal force and gravity, $\boldsymbol{D} = diag[d_1, d_2, \cdots, d_n]$ is matrix which means coefficients of joints' viscous friction and $\boldsymbol{\tau} \in \mathrm{R}^{n}$ is joint torque. The kinematic equation of a robot, that the relation between the i-th link's velocity $\dot{\boldsymbol{r}}_i \in \mathrm{R}^{m}$ and the angular velocity $\dot{\boldsymbol{q}} \in \mathrm{R}^{n}$ is represented by

$$\dot{\boldsymbol{r}}_i = \boldsymbol{J}_i\dot{\boldsymbol{q}} \qquad (i = 1, 2, \cdots, n) \qquad (2)$$

Here, $\boldsymbol{J}_i \in R^{m\times n}$ can be described as Jacobian matrix with zero block matrix, $\boldsymbol{J}_i = [\tilde{\boldsymbol{J}}_i,\ \boldsymbol{0}]$. By differentiating Eq. (2),

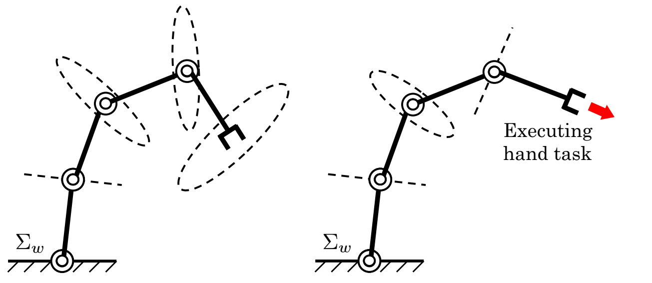

(a) Dynamic manipulability (DM) ellipses and segment

(b) Dynamic reconfiguration manipulability (DRM) ellipses and segments

Fig. 2. (a) Dynamic manipulability ellipsoids (DMEs) represent the possible accelerations for each link with no prior task and (b) dynamic reconfiguration manipulability ellipsoids (DRMEs) represent the possible accelerations for intermediate links during the system executing primary task.

we can obtain the following equation.

$$\ddot{\boldsymbol{r}}_i = \boldsymbol{J}_i(\boldsymbol{q})\ddot{\boldsymbol{q}} + \dot{\boldsymbol{J}}_i(\boldsymbol{q})\dot{\boldsymbol{q}} \tag{3}$$

where we can understand that $\dot{\boldsymbol{J}}_i(\boldsymbol{q})\dot{\boldsymbol{q}}$ is the acceleration as Coliolis and centrifugal acceleration resulted from nonlinear relation of two-coordinates-space represented by $\boldsymbol{q}_i$ to $\boldsymbol{r}_i$. Then, from Eqs. (1) and (3) we can obtain the following equation.

$$\ddot{\boldsymbol{r}}_i - \dot{\boldsymbol{J}}_i(\boldsymbol{q})\dot{\boldsymbol{q}} = \boldsymbol{J}_i\boldsymbol{M}^{-1}[\boldsymbol{\tau} - \boldsymbol{h}(\boldsymbol{q},\dot{\boldsymbol{q}}) - \boldsymbol{g}(\boldsymbol{q}) - \boldsymbol{D}\dot{\boldsymbol{q}}] \tag{4}$$

Here, two variables are defined as follows:

$$\tilde{\boldsymbol{\tau}} \triangleq \boldsymbol{\tau} - \boldsymbol{h}(\boldsymbol{q},\dot{\boldsymbol{q}}) - \boldsymbol{g}(\boldsymbol{q}) - \boldsymbol{D}\dot{\boldsymbol{q}} \tag{5}$$

$$\ddot{\tilde{\boldsymbol{r}}}_i \triangleq \ddot{\boldsymbol{r}}_i - \dot{\boldsymbol{J}}_i(\boldsymbol{q})\dot{\boldsymbol{q}} = \boldsymbol{J}_i(\boldsymbol{q})\ddot{\boldsymbol{q}} \tag{6}$$

So, Eq. (4) can be rewritten as

$$\ddot{\tilde{\boldsymbol{r}}}_i = \boldsymbol{J}_i\boldsymbol{M}^{-1}\tilde{\boldsymbol{\tau}} \qquad (i = 1, 2, \cdots, n) \tag{7}$$

Considering desired accelerations $\ddot{\tilde{\boldsymbol{r}}}_{id}$ of all links yielded by a set of joint torques $\tilde{\boldsymbol{\tau}}$ which satisfies an Euclidean norm condition, that is, $\|\tilde{\boldsymbol{\tau}}\| = (\tilde{\tau}_1^2 + \tilde{\tau}_2^2 + \cdots + \tilde{\tau}_n^2)^{1/2} \le 1$, each tip acceleration shapes an ellipsoid in range space of $\boldsymbol{J}_i$. These ellipsoids of each link have been known as "Dynamic Manipulability Ellipsoid (DME)" [2] (Fig.2(a)) which are described as

$$\ddot{\tilde{\boldsymbol{r}}}_{id}^T[\boldsymbol{J}_i(\boldsymbol{M}^T\boldsymbol{M})^{-1}\boldsymbol{J}_i^T]^+\ddot{\tilde{\boldsymbol{r}}}_{id} \le 1, \;\; and \;\; \ddot{\tilde{\boldsymbol{r}}}_{id} \in \mathrm{R}(\boldsymbol{J}_i) \tag{8}$$

where, $\mathrm{R}(\boldsymbol{J}_i)$ represents range space of $\boldsymbol{J}_i$.

B. Dynamic Reconfiguration Manipulability

Here we assume that the desired end-effector's acceleration $\ddot{\boldsymbol{r}}_{nd}$ is given as primary task. The relation between $\ddot{\tilde{\boldsymbol{r}}}_n$ and $\tilde{\boldsymbol{\tau}}$ is denoted to change i to n from Eq. (7), then,

$$\ddot{\tilde{\boldsymbol{r}}}_n = \boldsymbol{J}_n\boldsymbol{M}^{-1}\tilde{\boldsymbol{\tau}} \tag{9}$$

Solving Eq. (9) for $\tilde{\boldsymbol{\tau}}$ yielding desired acceleration $\ddot{\tilde{\boldsymbol{r}}}_{nd}$

$$\begin{aligned}\tilde{\boldsymbol{\tau}} = {} & (\boldsymbol{J}_n\boldsymbol{M}^{-1})^+\ddot{\tilde{\boldsymbol{r}}}_{nd} \\ & +[\boldsymbol{I}_n - (\boldsymbol{J}_n\boldsymbol{M}^{-1})^+(\boldsymbol{J}_n\boldsymbol{M}^{-1})]\,{}^1\boldsymbol{l}\end{aligned} \tag{10}$$

${}^1\boldsymbol{l}$ is an arbitrary vector satisfying ${}^1\boldsymbol{l} \in \mathrm{R}^n$. The left superscript "1" of ${}^1\boldsymbol{l}$ means the first dynamic reconfiguration task. In the right side of Eq. (10), the first term denotes the solution making $\tilde{\boldsymbol{\tau}}$ minimize in the null space of $\boldsymbol{J}_n\boldsymbol{M}^{-1}$ during implementing $\ddot{\tilde{\boldsymbol{r}}}_{nd}$. The second term denotes the components of torques at each joint, which can change the shape of manipulator regardless with the influence of $\ddot{\tilde{\boldsymbol{r}}}_{nd}$ given arbitrarily as end-effector acceleration for tracking the desired trajectory. Providing the first dynamic reconfiguration task, that is the first reconfiguration task ${}^1\ddot{\tilde{\boldsymbol{r}}}_{jd}$ $(j = 1, 2, \cdots, n{-}1)$, is given to the j-th link, shall we discuss realizability of ${}^1\ddot{\boldsymbol{r}}_{jd}$ in the following argument. In this research, ${}^1\ddot{\boldsymbol{r}}_{jd}$ is assumed to be commanded by an dynamic reconfiguration control system of higher level. We can obtain the relation of ${}^1\ddot{\tilde{\boldsymbol{r}}}_j$ and $\ddot{\tilde{\boldsymbol{r}}}_{nd}$ from Eqs. (7) and (10).

$$\begin{aligned}{}^1\ddot{\tilde{\boldsymbol{r}}}_j = {} & \boldsymbol{J}_j\boldsymbol{M}^{-1}(\boldsymbol{J}_n\boldsymbol{M}^{-1})^+\ddot{\tilde{\boldsymbol{r}}}_{nd} \\ & +\boldsymbol{J}_j\boldsymbol{M}^{-1}[\boldsymbol{I}_n - (\boldsymbol{J}_n\boldsymbol{M}^{-1})^+(\boldsymbol{J}_n\boldsymbol{M}^{-1})]\,{}^1\boldsymbol{l}\end{aligned} \tag{11}$$

Then, according to the relation of Eq. (6),

$$\begin{aligned}& {}^1\ddot{\boldsymbol{r}}_j - \dot{\boldsymbol{J}}_j\dot{\boldsymbol{q}} - \boldsymbol{J}_j\boldsymbol{M}^{-1}(\boldsymbol{J}_n\boldsymbol{M}^{-1})^+(\ddot{\boldsymbol{r}}_{nd} - \dot{\boldsymbol{J}}_n\dot{\boldsymbol{q}}) \\ & = \boldsymbol{J}_j\boldsymbol{M}^{-1}[\boldsymbol{I}_n - (\boldsymbol{J}_n\boldsymbol{M}^{-1})^+(\boldsymbol{J}_n\boldsymbol{M}^{-1})]\,{}^1\boldsymbol{l}\end{aligned} \tag{12}$$

Here, we define three variables shown as

$${}^1\ddot{\bar{\boldsymbol{r}}}_j \triangleq \dot{\boldsymbol{J}}_j\dot{\boldsymbol{q}} + \boldsymbol{J}_j\boldsymbol{M}^{-1}(\boldsymbol{J}_n\boldsymbol{M}^{-1})^+(\ddot{\boldsymbol{r}}_{nd} - \dot{\boldsymbol{J}}_n\dot{\boldsymbol{q}}) \tag{13}$$

$$\Delta\,{}^1\ddot{\boldsymbol{r}}_j \triangleq {}^1\ddot{\boldsymbol{r}}_j - {}^1\ddot{\bar{\boldsymbol{r}}}_j \tag{14}$$

$${}^1\boldsymbol{\Lambda}_j \triangleq \boldsymbol{J}_j\boldsymbol{M}^{-1}[\boldsymbol{I}_n - (\boldsymbol{J}_n\boldsymbol{M}^{-1})^+(\boldsymbol{J}_n\boldsymbol{M}^{-1})] \tag{15}$$

In Eq. (13), ${}^1\ddot{\bar{\boldsymbol{r}}}_j$ is represented for the acceleration caused by manipulator's shape-changing. In the right side of Eq. (13), the first term is denoted as the Coliolis and centrifugal acceleration of j-th link, and the second term is represented for the influence of ${}^1\ddot{\tilde{\boldsymbol{r}}}_{nd}$ on j-th link except Coliolis and centrifugal acceleration at n-th link because its acceleration is peculiar on its coordinate flame. So, Eq. (12) can be rewritten as

$$\Delta^1\ddot{\boldsymbol{r}}_j = {}^1\boldsymbol{\Lambda}_j\,{}^1\boldsymbol{l} \tag{16}$$

The relation between ${}^1\ddot{\boldsymbol{r}}_j$ and $\Delta^1\ddot{\boldsymbol{r}}_j$ is shown in Fig. 3. However, the problem is whether we can yield desired $\Delta^1\ddot{\boldsymbol{r}}_{jd}$, that is, whether we can find ${}^1\boldsymbol{l}$ to generate $\Delta^1\ddot{\boldsymbol{r}}_{jd}$. From Eq. (16), we can obtain ${}^1\boldsymbol{l}$ as

$${}^1\boldsymbol{l} = {}^1\boldsymbol{\Lambda}_j^+\Delta^1\ddot{\boldsymbol{r}}_{jd} + (\boldsymbol{I}_n - {}^1\boldsymbol{\Lambda}_j^+\,{}^1\boldsymbol{\Lambda}_j)\,{}^2\boldsymbol{l} \tag{17}$$

In Eq. (17), ${}^2\boldsymbol{l}$ is an arbitrary vector satisfying ${}^2\boldsymbol{l} \in \mathrm{R}^n$. Assuming that ${}^1\boldsymbol{l}$ is restricted as $\|{}^1\boldsymbol{l}\| \le 1$, then we obtain next relation,

$$(\Delta^1\ddot{\boldsymbol{r}}_{jd})^T({}^1\boldsymbol{\Lambda}_j^+)^{T\,1}\boldsymbol{\Lambda}_j^+\Delta^1\ddot{\boldsymbol{r}}_{jd} \le 1 \tag{18}$$

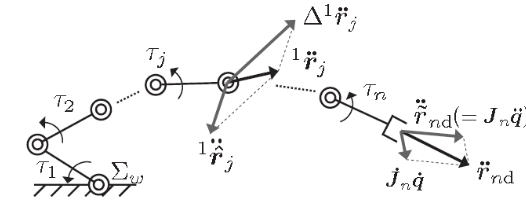

Fig. 3. Reconfiguration at intermediate link during hand task executed

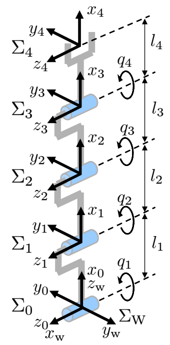

Fig. 4. Kinematical model

If $rank({}^1\boldsymbol{\Lambda}_j) = m$, Eq. (18) represents an ellipsoid expanding in m-dimensional space, holding

$$\Delta^1\ddot{\boldsymbol{r}}_{jd} = {}^1\boldsymbol{\Lambda}_j{}^1\boldsymbol{\Lambda}_j^+\Delta^1\ddot{\boldsymbol{r}}_{jd}, \quad \Delta^1\ddot{\boldsymbol{r}}_{jd} \in \mathrm{R}^m, \tag{19}$$

which indicates that $\Delta^1\ddot{\boldsymbol{r}}_{jd}$ can be arbitrarily generated in m-dimensional space and Eq. (16) always has the solution ${}^1\boldsymbol{l}$ corresponding to all $\Delta^1\ddot{\boldsymbol{r}}_{jd} \in \mathrm{R}^m$. On the other hand, if $rank({}^1\boldsymbol{\Lambda}_j) = r < m$, $\Delta\ddot{\boldsymbol{r}}_{jd}$ does not value arbitrarily in R^m. In this case, reduced $\Delta\ddot{\boldsymbol{r}}_{jd}$ is denoted as $\Delta^1\ddot{\boldsymbol{r}}^*_{jd}$. Then Eq. (18) is written as

$$\begin{aligned}(\Delta^1\ddot{\boldsymbol{r}}^*_{jd})^T({}^1\boldsymbol{\Lambda}_j^+)^T\,{}^1\boldsymbol{\Lambda}_j^+\Delta^1\ddot{\boldsymbol{r}}^*_{jd} \le 1 \\ (\Delta^1\ddot{\boldsymbol{r}}^*_{jd} = {}^1\boldsymbol{\Lambda}_j{}^1\boldsymbol{\Lambda}_j^+\Delta^1\ddot{\boldsymbol{r}}_{jd})\end{aligned} \tag{20}$$

Equation (20) describes an ellipsoid expanded in r-dimensional space. These ellipsoids of Eqs. (18) and (20) are shown in Fig.2(b).

C. Dynamic Reconfiguration Manipulability Shape Index (DRMSI)

In this section, we propose the index evaluating DRM. Thus, by applying the singular value decomposition for this matrix $\boldsymbol{\Lambda}$, we get

$${}^1\boldsymbol{\Lambda}_j ={}^1 \boldsymbol{U}_j^1\boldsymbol{\Sigma}_j^1\boldsymbol{V}_j^T \tag{21}$$

$${}^1\boldsymbol{\Sigma}_j = \begin{array}{c c} & \begin{array}{cc} r & \quad n-r \end{array} \\ \begin{array}{c} r \\ \\ m-r \end{array} & \left[\begin{array}{ccc|c} {}^1\sigma_{j,1} & & \boldsymbol{0} & \\ & \ddots & & \boldsymbol{0} \\ \boldsymbol{0} & & {}^1\sigma_{j,r} & \\ & \boldsymbol{0} & & \boldsymbol{0} \end{array}\right] \end{array} \tag{22}$$

In Eqs. (21) and (22), ${}^1\boldsymbol{U} \in \mathrm{R}^{m\times m}, {}^1\boldsymbol{V} \in \mathrm{R}^{n\times n}$ are orthogonal matrixes, and r denotes the number of non-zero singular values of ${}^1\boldsymbol{\Lambda}_j$ and $\sigma_{j,1} \ge \cdots \ge \sigma_{j,r} > 0$. In addition, $r \le m$ because $rank({}^1\boldsymbol{\Lambda}_j) \le m$. So, dynamic reconfiguration capability of j-th link when hand of manipulator operating task can be described by following equation.

$${}^1w_j ={}^1 \sigma_{j,1} \cdot{}^1 \sigma_{j,2} \cdots{}^1 \sigma_{j,r} \tag{23}$$

In this paper, we defined the value of w_j in Eq. (23) as dynamic reconfiguration manipulability measure (DRMM), which indicates the degree of that reconfiguration acceleration of j-th link can be generated for arbitrary direction. And, volume of dynamic reconfiguration ellipsoid at the j-th link is described as ${}^1V_{DRj}$. Then, in order to consider dynamic reconfiguration measure of the whole manipulator-links, we define a index named dynamic reconfiguration manipulability shape index (DRMSI) as follows:

$${}^1W_{DR} = \sum_{j=1}^{n-1} a_j \; {}^1V_{DRj} \tag{24}$$

Here, a_j is unit adjustment between different dimension. In this paper, singular-values increase a hundredfold to enlarge value of ellipsoid, compared to ellipse or line segment.

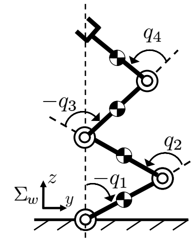

Fig. 5. Dynamical model

III. Models

To show and prove the feasibility of DRM, we construct a 4 links' redundant manipulator which works in 2-dimensional space. In this section, we will divide the model of the redundant manipulator into two parts-kinematical model and dynamical model, to introduce its structure.

A. Kinematical Model

In this section, we will introduce the kinematical model of 4 links' redundant manipulator. The model is shown in Fig.4, and coordinate transformations which based on Fig.4 are shown as follows. Here, we use S_i, C_i instead of $\sin q_i$, $\cos q_i$ to show ith-link's joint angle q_i.

$$\begin{aligned}{}^W\boldsymbol{T}_0 &= \begin{bmatrix} 0 & 0 & 1 & 0 \\ 0 & -1 & 0 & 0 \\ 1 & 0 & 0 & 0 \\ 0 & 0 & 0 & 1 \end{bmatrix}\begin{bmatrix} C_1 & -S_1 & 0 & 0 \\ S_1 & C_1 & 0 & 0 \\ 0 & 0 & 1 & 0 \\ 0 & 0 & 0 & 1 \end{bmatrix} \\ &= \begin{bmatrix} 0 & 0 & 1 & 0 \\ -S_1 & -C_1 & 0 & 0 \\ C_1 & -S_1 & 0 & 0 \\ 0 & 0 & 0 & 1 \end{bmatrix}\end{aligned} \tag{25}$$

$$\begin{aligned}{}^0\boldsymbol{T}_1 &= \begin{bmatrix} 1 & 0 & 0 & l_1 \\ 0 & 1 & 0 & 0 \\ 0 & 0 & 1 & 0 \\ 0 & 0 & 0 & 1 \end{bmatrix}\begin{bmatrix} C_2 & -S_2 & 0 & 0 \\ S_2 & C_2 & 0 & 0 \\ 0 & 0 & 1 & 0 \\ 0 & 0 & 0 & 1 \end{bmatrix} \\ &= \begin{bmatrix} C_2 & -S_2 & 0 & l_1 \\ S_2 & C_2 & 0 & 0 \\ 0 & 0 & 1 & 0 \\ 0 & 0 & 0 & 1 \end{bmatrix}\end{aligned} \tag{26}$$

$$\begin{aligned}{}^1\boldsymbol{T}_2 &= \begin{bmatrix} 1 & 0 & 0 & l_2 \\ 0 & 1 & 0 & 0 \\ 0 & 0 & 1 & 0 \\ 0 & 0 & 0 & 1 \end{bmatrix}\begin{bmatrix} C_3 & -S_3 & 0 & 0 \\ S_3 & C_3 & 0 & 0 \\ 0 & 0 & 1 & 0 \\ 0 & 0 & 0 & 1 \end{bmatrix} \\ &= \begin{bmatrix} C_3 & -S_3 & 0 & l_2 \\ S_3 & C_3 & 0 & 0 \\ 0 & 0 & 1 & 0 \\ 0 & 0 & 0 & 1 \end{bmatrix}\end{aligned} \tag{27}$$

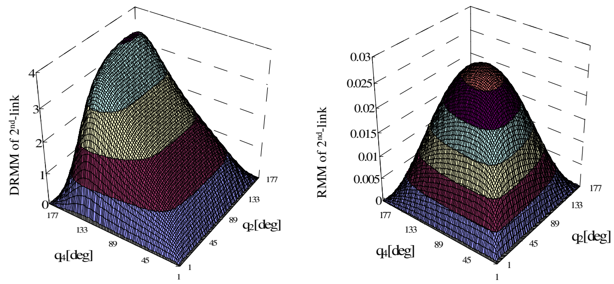

(a) 2nd-link's DRMM distribution (b) 2nd-link's RMM distribution

Fig. 6. 2nd-link's DRMM and RMM distribution

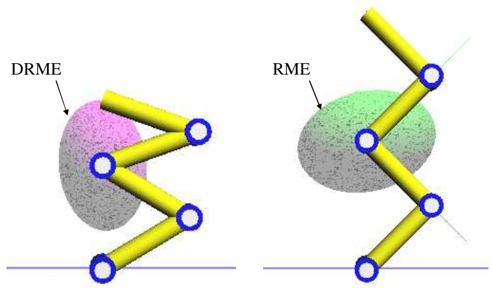

(a) (b)

Fig. 7. Shapes of manipulator: (a) shape of the peak of 2nd-link's DRMM with DRME, (b) shape of the peak of 2nd-link's RMM with RME

$$
{}^{2}\boldsymbol{T}_3 = \begin{bmatrix} 1 & 0 & 0 & l_3 \\ 0 & 1 & 0 & 0 \\ 0 & 0 & 1 & 0 \\ 0 & 0 & 0 & 1 \end{bmatrix} \begin{bmatrix} C_4 & -S_4 & 0 & 0 \\ S_4 & C_4 & 0 & 0 \\ 0 & 0 & 1 & 0 \\ 0 & 0 & 0 & 1 \end{bmatrix} = \begin{bmatrix} C_4 & -S_4 & 0 & l_3 \\ S_4 & C_4 & 0 & 0 \\ 0 & 0 & 1 & 0 \\ 0 & 0 & 0 & 1 \end{bmatrix} \tag{28}
$$

$$
{}^{3}\boldsymbol{T}_4 = \begin{bmatrix} 1 & 0 & 0 & l_4 \\ 0 & 1 & 0 & 0 \\ 0 & 0 & 1 & 0 \\ 0 & 0 & 0 & 1 \end{bmatrix} \begin{bmatrix} 1 & 0 & 0 & 0 \\ 0 & 1 & 0 & 0 \\ 0 & 0 & 1 & 0 \\ 0 & 0 & 0 & 1 \end{bmatrix} = \begin{bmatrix} 1 & 0 & 0 & l_4 \\ 0 & 1 & 0 & 0 \\ 0 & 0 & 1 & 0 \\ 0 & 0 & 0 & 1 \end{bmatrix} \tag{29}
$$

B. Dynamical Model

The dynamical model of 4-links manipulator is shown in Fig.5. Length, mass and coefficient of viscous friction of each link and joint are set to be 0.3[m], 1.0[kg], and 2.0[N·m·s/rad]. The barycentre of each link is set to the centre of each link.

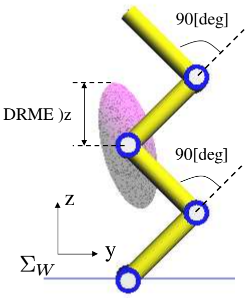

Fig. 8. (DRME)z of 2nd link

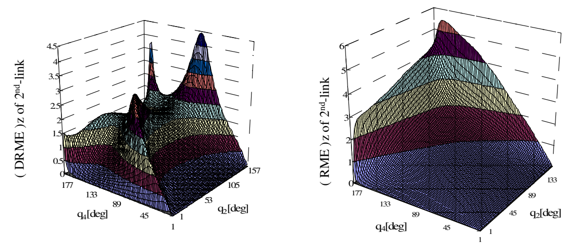

(a) (b)

Fig. 9. (a) Vertical acceleration derived from DRME, (b) Vertical velocity derived from RME

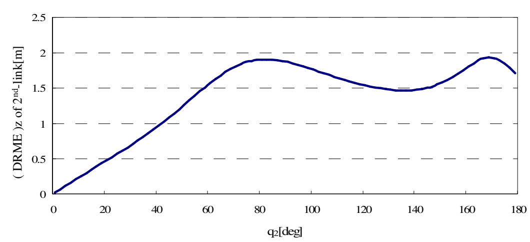

Fig. 10. (DRME)z when $q_4 = 130$[deg]

IV. Simulations

In this section, we use a 4-links redundent manipulator which works in 2-dimentional space to confirm the physical properties of DRM, and prove the validity and usefulness of DRM. In these simulations, we assume that tip of 2nd link and 4th link are always placed $y = 0$ in initial position, that is, when q_2 and q_4 are given, q_1 and q_3 are set as $q_1 = -q_2/2.0$ and $q_3 = -(q_2 + q_4)/2.0$.

A. Simulation of DRMM

In this simulation, we checked DRMM of each configuration of the manipulator when the acceleration of tip of end link is given, and compared it with Reconfiguraton manipulability Measure(RMM). Fig.6 shows each configuration's distribution of 2nd-link's DRMM and RMM.

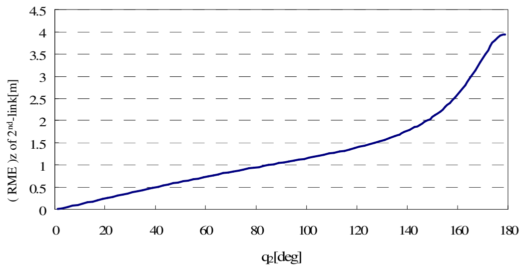

Fig. 11. (RME)z when $q_4 = 130$[deg]

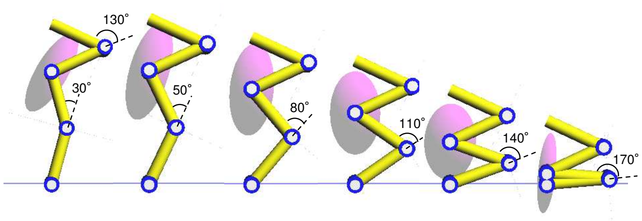

Fig. 12. DRME of various configurations ($q_4 = 130[deg]$)

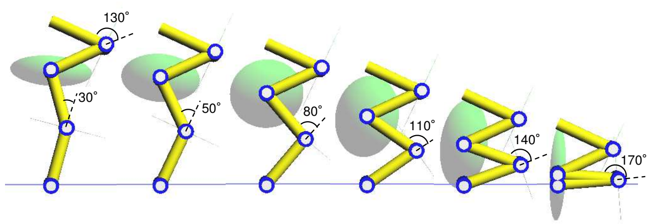

Fig. 13. RME of various configurations ($q_4 = 130[deg]$)

From Fig.6, we can find that when $q_2 = 90°$, $q_4 = 90°$, the value of RMM is maximum, and when $q_2 = 118°$, $q_4 = 141°$, the value of DRMM is maximum. The shapes of those time are shown in Fig.7. From Fig.6, we can see the shape of DRMM's peak has a little curved. We think the reason causing this configuration is that we put dynamics into consideration, and the masses of the links have large influence to manipulability.

B. Verification simulation based on DRM

According to former researches we can know that the condition of manipulator's manipulability can be seen by the volumes of ellipsoids we made. For example, the concept of Reconfiguration Manipulability Measure said that, when the ellipsoid turns to be sphere, the reconfiguration ability becomes the best. But to DRME, the ability is not only that but also depend on the task that manipulators do. So, in this simulation, we defined the length of DRME in z-direction as (DRME)z like Fig.8, and made a task to keep the 3rd and 4th links' configuration and keep them right above the 1st link. Meanwhile, let the tip of 4th link move to find the value of 2nd link's acceleration in z-direction.

Each configuration's (DRME)z and (RME)z are shown in Fig.9. We can see that the distribution of (RME)z increases monotonically with the raising of joint degree. However, the distribution of (DRME)z has many peaks. So, we keep $q_4 = 130$[deg] from Fig.9 and had the relationship shown in Fig.10 and Fig.11. Meanwhile, various configurations of the manipulator in this condition are shown in Fig.12 and Fig.13.

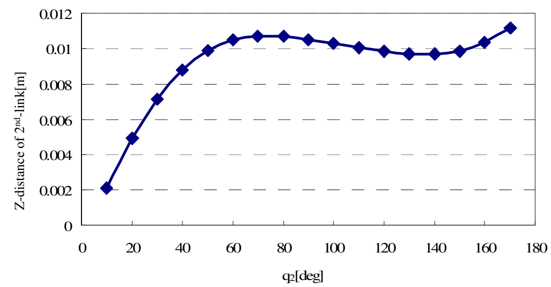

Fig. 14. Z-direction's moving distance of 2nd-link

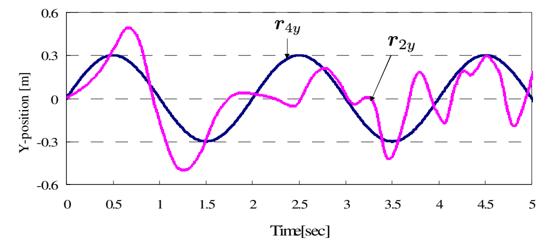

Fig. 15. Y-direction's moving distances

At the same time, with the raising of q_2, z-direction's moving distance of 2nd link turns larger from $0°$ to $80°$, and then drops from $80°$ to $140°$, and raises at last. The relation between them is shown in Fig.14. Trend showed in Fig.14 is similar to that of Fig.10. According to this result, we can prove the validity and usefulness of DRM.

C. Shape-changing simulation when acceleration of 4th-link's tip is given

In this section, we set 4th-link's tip have periodic motion, to check manipulator's shape-changing basing on DRM. Based on eq.(10), we set the acceleration of 4th-link's tip and input torque as follows:

$$\ddot{\boldsymbol{r}}_{4d} = \begin{bmatrix} -\alpha(2\pi/T)^2 \sin(2\pi/T)t \\ 0 \end{bmatrix}, \ {}^1\boldsymbol{l} = \begin{bmatrix} 2 \\ 2 \\ 2 \\ 2 \end{bmatrix} \tag{30}$$

Here, we set $T = 2.0[sec]$, $\alpha = 0.3[m]$. The initial angle of each link is shown in Fig.(8), where $q_1 = -q_2/2$, and $q_4 = -(q_2 + q_4)/2$, and the initial angular velocity of each link is set to 0.

Y-direction's moving distances of 2nd-link and 4th-link are shown in Fig.15, and z-direction's moving distances of 2nd-link and 4th-link are shown in Fig.16. Meanwhile, the screen-shot of 4-links manipulators when 4th link's tip is doing

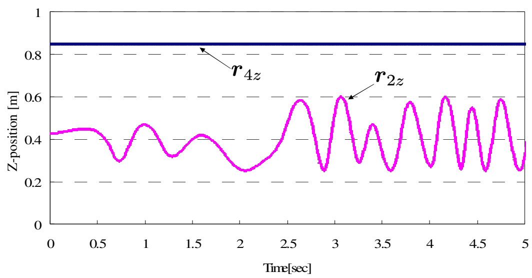

Fig. 16. Z-direction's moving distances

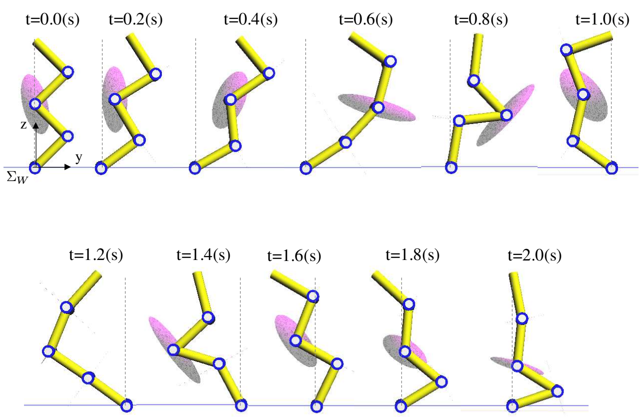

Fig. 17. Screen-shot of periodic motion

periodic motion in one cycle is given by Fig.17. From Fig.17, what the Fig.15 and 16 show can be seen clearly. In addition, from Fig.17, we can hardly see the shape of ellipsoid when $t = 1.2(s)$ because the dynamic reconfiguration capability of 2nd-link at that time is very low.

In this simulation, whatever the value of input torque ${}^1\boldsymbol{l}$ changes, it will never have any influences to manipulator's hand's motion.

V. Conclusion

In this paper, we proposed a new index named Dynamic Reconfiguration Manipulability(DRM) that represents how much the dynamical system of robots possesses the ability to generate acceleration for shape-reconfiguration in workspace by unit torque input for all joints during executing primary tasks. Then, we have shown simulations to indicate the physical properties of DRM, and proved validity and usefulness of DRM. What I want to emphasize is that, this research was just been proposed, and it has broad space to be extended. For the future work, we plan to add DRM into 7-links manipulators such as PA-10(produced by Mitsubishi Heavy Industries, Ltd.) for trajectory tracking and grinding tasks. We aim to improve manipulators' accuracy given to tasks and find the optimum configurations through whole processes. Furthermore, we intend to apply DRM to humanoid robot to analyse humanoid robot's walking states.

Acknowledgment

First, we would like to give deepest appreciation to the writters listed in references for their excellent papers, and we would also like to thank this conference for giving us chances to report our research. The way of research is endless and we will optimize our research in the future.

References

[1] T. Yoshikawa, "Manipulability of Robotic Mechanisms," *The International Journal of Robotics Research*, Vol. 4, No. 2, pp. 3-9, 1985.

[2] T. Yoshikawa, "Dynamic Manipulability of Robot Manipulators," *Proceedings of the IEEE International Conference on Robotics and Automation*, Vol. 2, No. 1, pp. 113-124, 1985.

[3] R. Koeppe and T.Yoshikawa, "Dynamic manipulability analysis of compliant motion," *Proceedings of the IEEE/RSJ International Conference on Intelligent Robots and Systems ' 97*, 1997.

[4] M. Minami, Y. Nomura and T. Asakura, "Avoidance Manipulability for Redundant Manipulators," *Journal of the Robotics Society of Japan*, Vol. 17, No. 6, pp. 887-895, 1999 (in Japanese).

[5] M. Minami, J. Agubanhan, T. Asakura, "Robust Scene Recognition using a GA and Real-world Raw-image," *Measurement*, Vol. 29, pp. 249-267, 2001.

[6] Tsuneo Yoshikawa, "Foundations of Robot Control", CORONA PUBLISHING CO., LTD.,1988.

[7] Pasquale Chiacchio, "A new dynamic manipulability ellipsoid for redundant manipulators," *Robotica*, vol. 18, no. 4, pp. 381-387,2000.

[8] Keith L. Doty, Claudio Melchiorri, Eric M. Schwartz, and Claudio Bonivento, "Robot manipulability," *IEEE Transactions on Robotics and Automation*, vol. 11, no. 3, pp. 462-468, 1995.

[9] Timothy J. Graettinger and Bruce H. Krogh, "The acceleration radius: a global performance measure for robotic manipulators,"*IEEE Journal of Robotics and Automation*, vol. 4, no. 1, pp. 60-69, 1988.

[10] Michael T. Rosenstein, Roderic A. Grupen, "Velocity-Dependent Dynamic Manipulability," *International Conference on Robotics and Automation - ICRA*, pp. 2424-2429, 2002.

[11] K.L.Doty,C.Melchiorri,E.M.Schwartz,C.Bonivento, "Robot Manipulability,"*IEEE Transactions on Robotics and Automation - IEEE TRANS ROBOTICS AUTOMAT*, vol. 11, no. 3, pp. 462-468, 1995.